Platinum Clusters

Deutsche Ausgabe: DOI: 10.1002/ange.201604903
Internationale Ausgabe: DOI: 10.1002/anie.201604903

Monomeric Chini-Type Triplatinum Clusters Featuring Dianionic and Radical-Anionic π*-Systems

*Brandon R. Barnett, Arnold L. Rheingold, and Joshua S. Figueroa**

Dedicated to Professor Christopher C. Cummins on the occasion of his 50th birthday

Abstract: *Owing to their unique topologies and abilities to self-assemble into a variety of extended and aggregated structures, the binary platinum carbonyl clusters $[Pt_3(CO)_6]_n^{2-}$ ("Chini clusters") continue to draw significant interest. Herein, we report the isolation and structural characterization of the trinuclear electron-transfer series $[Pt_3(\mu\text{-}CO)_3(CNAr^{Dipp2})_3]^{n-}$ ($n = 0, 1, 2$), which represents a unique set of monomeric Pt_3 clusters supported by π-acidic ligands. Spectroscopic, computational, and synthetic investigations demonstrate that the highest-occupied molecular orbitals of the mono- and dianionic clusters consist of a combined π*-framework of the CO and $CNAr^{Dipp2}$ ligands, with negligible Pt character. Accordingly, this study provides precedent for an ensemble of carbonyl and isocyanide ligands to function in a redox non-innocent manner.*

Highly reduced carbonyl metalates have long interested organometallic chemists owing to their ability to place a relatively electropositive transition-metal center in a formally negative oxidation state.[1,2] This phenomenon is made possible in large part due to the strong π-acidic properties of the carbonyl ligand and has allowed for the isolation of many mono- and multi-nuclear binary carbonyl metalates from most members of the transition series.[3–6] With regard to topology and electronic structure, one of the most intriguing classes of such complexes are the so-called "Chini clusters," $[Pt_3(CO)_6]_n^{2-}$.[6–8] In these clusters, *triangulo*-Pt_3 units bearing both terminal and bridging carbonyl ligands stack one on top of the other along a common C_3 axis to form columnar structures bearing an overall doubly anionic charge. The higher nuclearity oligomers ($n = 5$–8) can self-assemble into continuous chains, with the dimensionality of long-range ordering being highly dependent upon the identity of the charge-balancing cations.[9–11] Many of the higher ordered structures display remarkable conductive properties, leading to interest in their use as tunable conductive materials based off of a molecular platform.[12,13] As such, a furthered understanding of the electronic structure and reactivity profiles available to these clusters continues to be of importance.[14]

While the oligomeric members of $[Pt_3(CO)_6]_n^{2-}$ with $n =$ 2–8 have all been isolated and structurally characterized,[7–11,15] the parent species $[Pt_3(CO)_6]^{2-}$ ($n = 1$) has eluded complete characterization. Although reportedly synthesized in situ via reduction of $[Pt_3(CO)_6]_2^{2-}$ with Na/K alloy, it could not be crystallized or precipitated from solution, with characterization relying solely upon IR and atomic absorption spectroscopies. Interestingly, although several mixed carbonyl/phosphine clusters of the type $Pt_3(\mu\text{-}CO)_3(PR_3)_3$ have been long-known,[16–20] their reduction to the corresponding platinates has not been reported, potentially implying that the weak π-accepting properties of triorganophosphines are insufficient to stabilize the presence of two negative charge equivalents.[21] Given our success in isolating isocyano analogues to classical carbonyl metalates using sterically encumbering *m*-terphenyl isocyanides,[22–25] we report herein the synthesis and structural characterization of $K_2[Pt_3(\mu\text{-}CO)_3(CNAr^{Dipp2})_3]$ ($Ar^{Dipp2} = 2,6\text{-}(2,6\text{-}(i\text{-}Pr)_2C_6H_3)_2C_6H_3$), as well as the open-shell monoanion $K[Pt_3(\mu\text{-}CO)_3(CNAr^{Dipp2})_3]$. These anionic clusters serve as isolobal mimics to $[Pt_3(CO)_6]^{2-}$ as well as putative $[Pt_3(CO)_6]^{\bullet-}$, with the highest occupied orbital shown to be primarily located on the ligand π* framework. Occupation of this highly delocalized π-symmetric orbital results in the aggregate set of isocyanide and carbonyl ligands functioning in a redox non-innocent fashion akin to multidentate redox active ligands.[26–28]

Exposure of a diethyl ether solution of two-coordinate $Pt(CNAr^{Dipp2})_2$[29,30] to 1 atm CO gas results in displacement of one isocyanide ligand and aggregation to afford the trinuclear cluster $Pt_3(\mu\text{-}CO)_3(CNAr^{Dipp2})_3$ (**1**, Scheme 1). Despite the presence of excess CO, further CO-for-isocyanide substitution is not observed even upon stirring for several days. Crystallographic characterization of **1** (Figure 1 A) reveals an equilateral *triangulo*-Pt_3 core with Pt–Pt distances (mean = 2.6496(2) Å) similar to those seen for $Pt_3(\mu\text{-}CO)_3(PR_3)_3$.[16–20] Trinuclear **1** adopts nearly ideal D_{3h} site symmetry, with the Pt–CO and Pt–CNR bond vectors all essentially coincident with the Pt_3 plane (maximum torsion angle = 8.56°). In accordance with its high symmetry in the solid state, the solution FTIR spectrum of **1** displays only a single ν(C≡N) and ν(C=O) mode (2118 and 1834 cm^{-1}, respectively; E' symmetric in the D_{3h} point group).

Remarkably, cyclic voltammetry of **1** in THF (Figure S3.1 in the Supporting Information) shows the presence of two reversible reduction events centered at −1.95 V ($\Delta E_p =$ 86 mV) and −2.60 V ($\Delta E_p = 81$ mV) versus Fc ($Fc = [(\eta^5\text{-}C_5H_5)_2Fe]$), suggesting the accessibility of the anionic clusters $[Pt_3(\mu\text{-}CO)_3(CNAr^{Dipp2})_3]^{n-}$ ($n = 1$, 2). Chemical reduction of

[*] B. R. Barnett, Prof. A. L. Rheingold, Prof. J. S. Figueroa
Department of Chemistry and Biochemistry
University of California, San Diego
9500 Gilman Drive MC 0358, La Jolla, CA 92193 (USA)
E-mail: jsfig@ucsd.edu

Supporting information for this article can be found under: http://dx.doi.org/10.1002/anie.201604903.

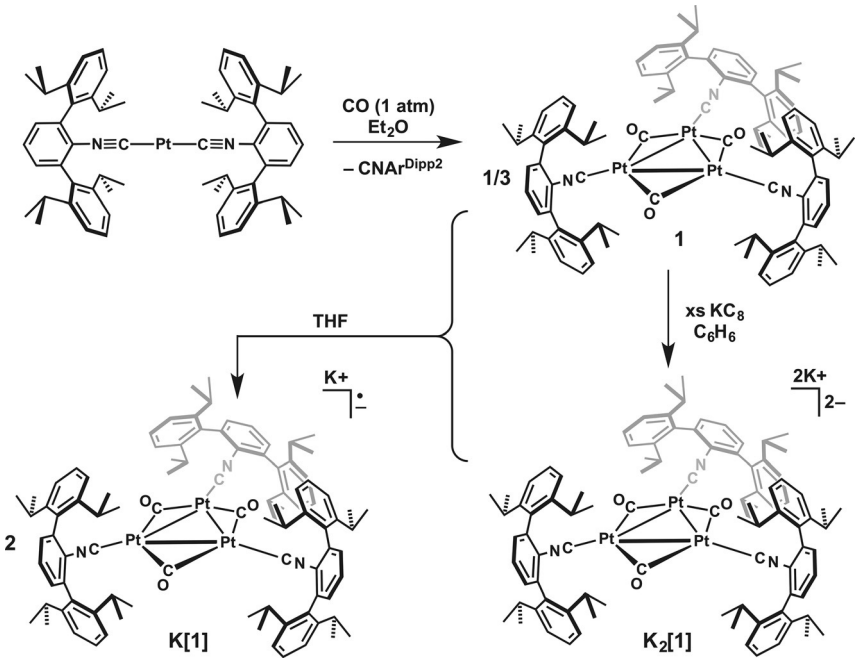

Scheme 1. Synthesis of clusters **1**, K[**1**], and K_2[**1**].

1 in benzene solution using an excess of KC_8 results in smooth formation of a deep purple diamagnetic product as assayed by ^{1}H and ^{13}C{^{1}H} NMR spectroscopy and proposed to be $K_2[Pt_3(\mu\text{-}CO)_3(CNAr^{Dipp2})_3]$ (K_2[**1**]; Scheme 1). Retention of the *triangulo*-$Pt_3(\mu\text{-}CO)_3(CNR)_3$ motif is suggested by peaks at $\delta = 242.2$ and $\delta = 194.5$ ppm in the ^{13}C{^{1}H} NMR spectrum corresponding to bridging carbonyl and terminal isocyanide ligands, respectively. This new species gives rise to a ^{195}Pt NMR signal at $\delta = -4271$ ppm, which is strikingly similar to that of **1** ($\delta = -4319$ ppm) given the wide chemical shift range inherent in ^{195}Pt NMR.[31] FTIR spectra in C_6D_6 show a single ν(C=O) band at 1722 cm^{-1}, as well as broad ν(C≡N) stretching modes centered at 2043 and 1985 cm^{-1}. These bands are shifted to significantly lower energies relative to **1** and can be compared with the bridging and terminal ν(CO) modes reported for in situ gener-

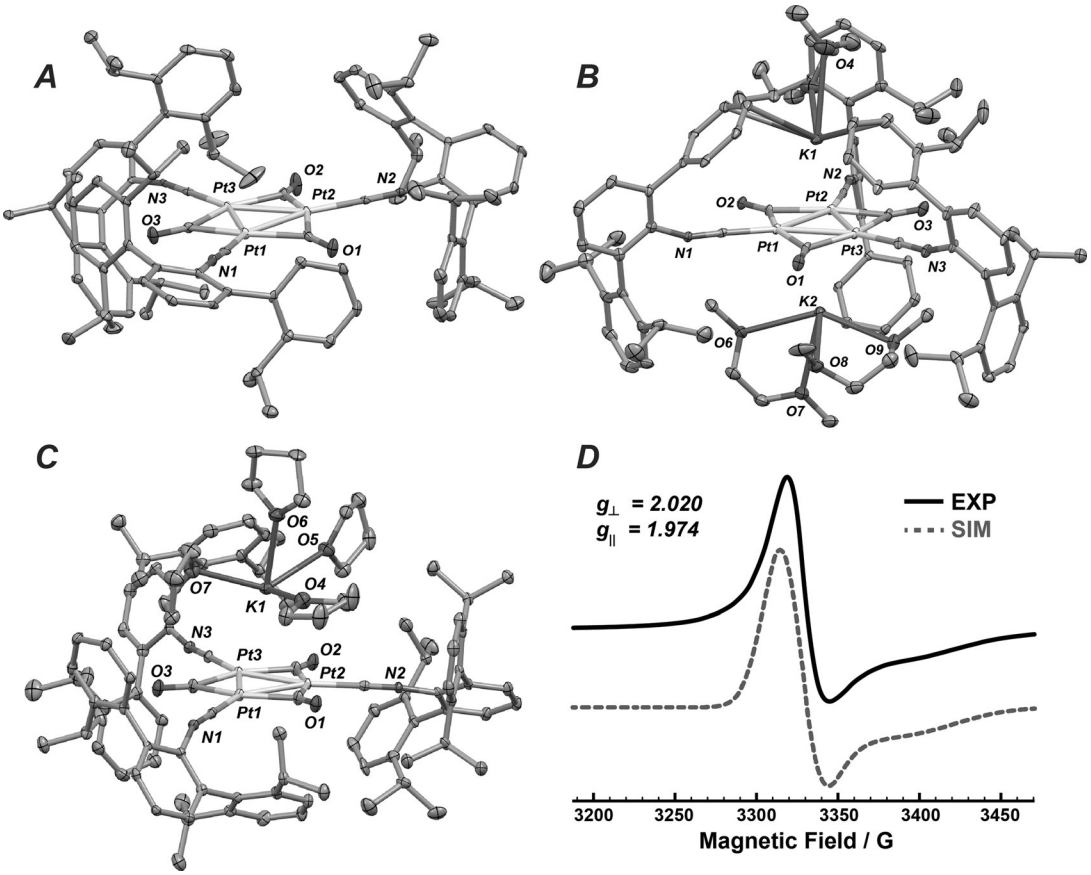

Figure 1. Molecular structures of **1** (A), $[K_2(DME)_3]$[**1**] (B) and $[K(THF)_4]$[**1**] (C). Some *iso*-propyl groups have been removed for clarity. D) Experimental (black) and simulated (gray-dashed) X-band powder EPR spectrum of $K(THF)_4$[**1**] recorded at 294 K.

ated $[Pt_3(CO)_6]^{2-}$ (1945, 1740 cm^{-1}, THF).[8]

Structure determination on single crystals of K_2[**1**] grown from DME/*n*-hexane at −35 °C confirmed the identity of this species to be the dianion $K_2(DME)_3[Pt_3(\mu\text{-}CO)_3(CNAr^{Dipp2})_3]$ ($K_2(DME)_3$[**1**], Figure 1 B). Each Pt_3 unit exists as a discreet entity and no oligomerization to higher nuclearity, stacked structures is observed. Most notably, despite the introduction of two negative charge equivalents, the structural features of the $[Pt_3(\mu\text{-}CO)_3(CNAr^{Dipp2})_3]$ core in $K_2(DME)_3$[**1**] are essentially unchanged relative to **1**. The Pt−C bond vectors remain nearly coincident with the Pt_3 plane, with only very minor perturbations of the Pt−Pt, Pt−C_{CNR}, and Pt−C_{CO} distances apparent (Table 1). The two potassium counterions sit directly over the centroid on either face of the Pt_3 triangle and are chelated by one or two molecules of DME.

Table 1: Selected bond lengths from the solid-state structures of complexes **1**, $K(THF)_4$[**1**], and $K_2(DME)_3$[**1**].

Complex	Mean *d*(Pt-Pt) [Å]	Mean *d*(Pt-C_{CNR}) [Å]	Mean *d*(Pt-C_{CO}) [Å]
1	2.6496(2)	1.917(3)	2.062(2)
$K(THF)_4$[**1**]	2.6448(3)	1.924(6)	2.047(4)
$K_2(DME)_3$[**1**]	2.6359(2)	1.896(4)	2.044(3)

In contrast to Chini's $[Pt_3(CO)_6]^{2-}$,[8] K_2[**1**] exhibits remarkable kinetic stability. As a solid, it can be stored for weeks in a glovebox freezer at −35 °C without change, while [D_6]benzene solutions of K_2[**1**] at 25 °C undergo decomposition over the course of several weeks to give free $CNAr^{Dipp2}$ as the sole isocyanide-containing species according to ^{1}H NMR spectroscopy. This kinetic stability results in an exceedingly simple synthetic method whereby analytical quality K_2[**1**] can be obtained in excellent yields (99 %) via simple lyophilization of the benzene solvent after filtration of the reaction mixture.

While Chini clusters of many nuclearities have been isolated, a common feature among all of them is an overall charge of 2−. Their reactions with oxidizing agents have been proposed to proceed via single-electron transfer to transiently form $[Pt_3(CO)_6]_n^{\bullet-}$, followed by dimerization and further aggregation to yield $[Pt_3(CO)_6]_{2n}^{2-}$ stacked clusters.[32] However, such monoradical species have not been observed to date during the course of these oxidations. The apparent resistance of $K_2[Pt_3(\mu\text{-}CO)_3(CNAr^{Dipp2})_3]$ (K_2[**1**]) toward aggregation, as well as the clean electrochemical data for **1**, suggested the potential accessibility of the open-shell monoanion $[Pt_3(\mu\text{-}CO)_3(CNAr^{Dipp2})_3]^{\bullet-}$. Accordingly, simple comproportionation of **1** and K_2[**1**] in [D_8]THF (Scheme 1) produces a dark green solution, which gives rise to only broad ^{1}H NMR signals indicative of the presence of a paramagnetic species ($\mu_{eff} = 1.7(2)\ \mu_B$, Evans method). Analysis by FTIR spectroscopy shows ν(C=O) (1775 cm^{-1}) and ν(C≡N) (2061, 2022 cm^{-1}) bands intermediate in energy with respect to those of **1** and K_2[**1**]. Storage of this solution at −35 °C yields black crystals of $K(THF)_4[Pt_3(\mu\text{-}CO)_3(CNAr^{Dipp2})_3]$ ($K(THF)_4$[**1**]) as determined by X-ray diffraction (Figure 1 C). As noted for $K_2(DME)_3$[**1**], the anionic fragment in $K(THF)_4$[**1**] is essentially isostructural to that of neutral **1** (Table 1). The coordination geometry about each platinum center remains almost perfectly planar, while the Pt−Pt, Pt−C_{CNR}, and Pt−C_{CO} bond lengths are basically unchanged from those in **1** and $K_2(DME)_3$[**1**] (Table 1). The room temperature solid-state EPR spectrum of $K(THF)_4$[**1**] displays axial symmetry, with $g_\perp = 2.020$ and $g_\parallel = 1.974$ (Figure 1 D). The small degree of *g* anisotropy and the minimal deviation of these values from 2.002 (*g* of a free electron) differ from EPR spectra typically seen for Pt-based $S = 1/2$ metalloradicals.[33–35] However, they are very much in accord with spectra exhibited by systems containing closed-shell platinum centers bound to radical ligands.[36,37] Noticeably, no coupling to the ^{195}Pt nucleus ($I = 1/2$, 33.8 % abundant) is resolved, suggesting that minimal spin density resides at the Pt_3 core.

Density Functional Theory (DFT) studies were undertaken in order to interrogate the electronic structure of the clusters $[Pt_3(\mu\text{-}CO)_3(CNAr^{Dipp2})_3]^{n-}$ ($n = 0$, 1, 2). The optimized geometries of the truncated models $[Pt_3(\mu\text{-}CO)_3(CNAr^{Ph2})_3]^{n-}$ ($[\mathbf{1}^*]^{n-}$, $n = 0$, 1, 2) satisfactorily reproduce the important metrical parameters of the corresponding structurally characterized triplatinum clusters **1**, $K(THF)_4$[**1**] and $K_2(DME)_3$[**1**] (Figures S4.1–3 and Tables S4.1–3). Remarkably, the calculated HOMO of $[\mathbf{1}^*]^{2-}$ (Figure 2 A)

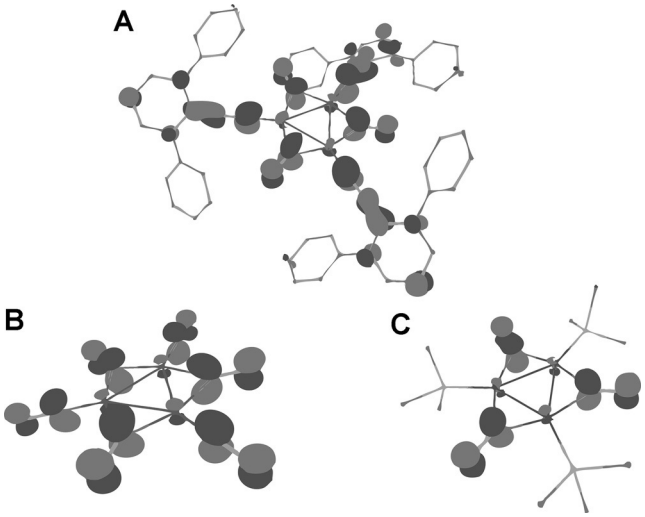

Figure 2. DFT Calculated HOMOs of $[\mathbf{1}^*]^{2-}$ (A), $[Pt_3(CO)_6]^{2-}$ (B), and $[Pt_3(\mu\text{-}CO)_3(PMe_3)_3]^{2-}$ (C). BP86/def2-TZVP/ZORA.

and SOMO of $[\mathbf{1}^*]^-$ consist of the in-phase combination of the out-of-plane π* orbitals of the carbonyl and isocyanide ligands (a_2'' in D_{3h} symmetry) with only a modest contribution from Pt-based orbitals (20.5 % for $[\mathbf{1}^*]^{2-}$ HOMO; 25.7 % for $[\mathbf{1}^*]^-$ SOMO).[38] The primarily ligand-based parentage of this orbital is in accord with the minimal shortening of the Pt−C bond distances upon reduction of **1** (Table 1), despite the sizeable shift of the IR ν(C=O) and ν(C≡N) bands to lower energies, which are usually attributable to increased metal-to-ligand π-backdonation. It is also consistent with semi-empirical extended Hückel calculations on $[Pt_3(CO)_6]^{2-}$, which predict a HOMO that is primarily CO π* in charac-

ter.[39–41] Indeed, DFT calculations on $[Pt_3(CO)_6]^{2-}$ yield a HOMO that is entirely analogous to that of $[\mathbf{1}^*]^{2-}$, namely the a_2'' combination of bridging and terminal CO out-of-plane π* orbitals (Figure 2B). This confirms that $K_2[\mathbf{1}]$ indeed functions as an isolobal analogue of $[Pt_3(CO)_6]^{2-}$, while $K[\mathbf{1}]$ is isolobal with the monoanion $[Pt_3(CO)_6]^{\bullet-}$, a putative fleeting intermediate in the oxidation of $[Pt_3(CO)_6]^{2-}$ to $[Pt_3(CO)_6]_2^{2-}$. The all-π-acid ligand sets employed in $K_2[\mathbf{1}]$ and $[Pt_3(CO)_6]^{2-}$ can be contrasted with the hypothetical dianions of the phosphine-substituted triplatinum clusters $Pt_3(\mu\text{-}CO)_3(PR_3)_3$.[16–20] DFT calculations for $[Pt_3(\mu\text{-}CO)_3(PMe_3)_3]^{2-}$ illustrate that the primarily σ-donating nature of the trimethylphosphine ligands precludes delocalization of electron density onto the terminal ligands in the cluster. For this complex, the HOMO is again a_2''-symmetric, but consists primarily of the out-of-plane π* orbitals of the bridging carbonyl ligands (Figure 2C). The relative localization of electron density onto the bridging ligands in $[Pt_3(\mu\text{-}CO)_3(PMe_3)_3]^{2-}$, along with the strongly σ-donating nature of the phosphine ligands, likely renders the reduction of $Pt_3(\mu\text{-}CO)_3(PR_3)_3$ to the corresponding dianion more difficult than the reduction of **1** to $K_2[\mathbf{1}]$, and serves to highlight the central role played by the all-π-acid ligand sets of $K_2[\mathbf{1}]$ and $[Pt_3(CO)_6]^{2-}$ in stabilizing the negative charge equivalents.

Interestingly, the modest contribution of platinum-based atomic orbitals to the a_2''-symmetric HOMO of $[\mathbf{1}^*]^{2-}$ is mostly $6p_z$ in parentage, while the molecular orbital contains only 0.8% 5d character. Similarly small 5d contributions are apparent in the SOMO of $[\mathbf{1}^*]^-$ (1.3% 5d) and the HOMO of $[Pt_3(CO)_6]^{2-}$ (1.4% 5d), an effect we believe can be traced to the intratriangular Pt–Pt bonding interactions.[42] Indeed, the only symmetry-adapted linear combination of Pt 5d orbitals for the $[Pt(\mu\text{-}CO)_3L_3]$ (L = CO, CNR) fragment with a_2'' symmetry (Figure S4.6–8) has significant Pt–Pt bonding character, which serves to significantly lower it in energy. Importantly, the resulting energy gap between these d orbitals and the a_2''-symmetric π* manifold is substantial (4.40–4.54 eV), which precludes significant orbital mixing. Remarkably, owing to the primarily ligand-based nature of the a_2'' HOMO/SOMO found for $[\mathbf{1}^*]^{2-}$ and $[\mathbf{1}^*]^-$, it can be noted that population of this orbital in $K_2[\mathbf{1}]$ and $K[\mathbf{1}]$ results in the CO/$CNAr^{Dipp2}$ ligand set acting in a formally redox non-innocent fashion. Distinct from these ligands merely functioning as π-acids, the successive reduction on going from **1** to $K(THF)_4[\mathbf{1}]$ and $K_2[\mathbf{1}]$ yields clusters best described as containing a $(Pt_3)^0$ core supported by a ligand set that, as an aggregate, bears a singly- or doubly-reduced π*-manifold. In essence, combining the out-of-plane π* orbitals of all six ligands in-phase renders them accessible in energy, allowing the a_2'' orbital to function as an electron reservoir reminiscent of multidentate redox non-innocent ligand systems bearing extended π-systems.[26]

The robust and highly-reduced nature of $K_2[Pt_3(\mu\text{-}CO)_3(CNAr^{Dipp2})_3]$ ($K_2[\mathbf{1}]$) allows it to undergo well-defined reactivity with main-group and transition-metal electrophiles (Scheme 2). Addition of a benzene solution of Ph_3SnCl or Et_3SiCl to $K_2[\mathbf{1}]$ proceeds with elimination of KCl and formation of the diamagnetic triplatinum clusters $K[Pt_3(\mu_3\text{-}SnPh_3)(\mu\text{-}CO)_3(CNAr^{Dipp2})_3]$ (**2**, Figure 3A) or $K[Pt_3(SiEt_3)(\mu\text{-}CO)_3(CNAr^{Dipp2})_3]$ (**3**, Figure 3B) as determined by X-ray diffraction. In **2**, the triphenylstannyl ligand is bound in a μ_3 fashion, a binding mode that is unprecedented for triorga-

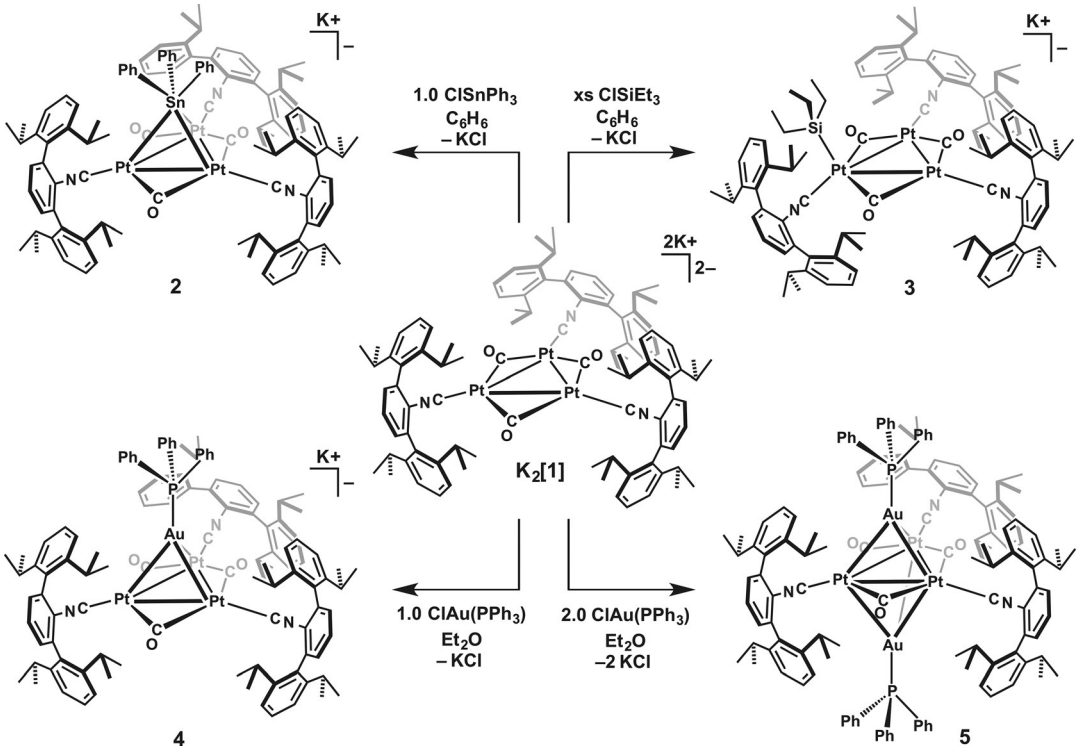

Scheme 2. Reactivity of $K_2[\mathbf{1}]$ with electrophiles.

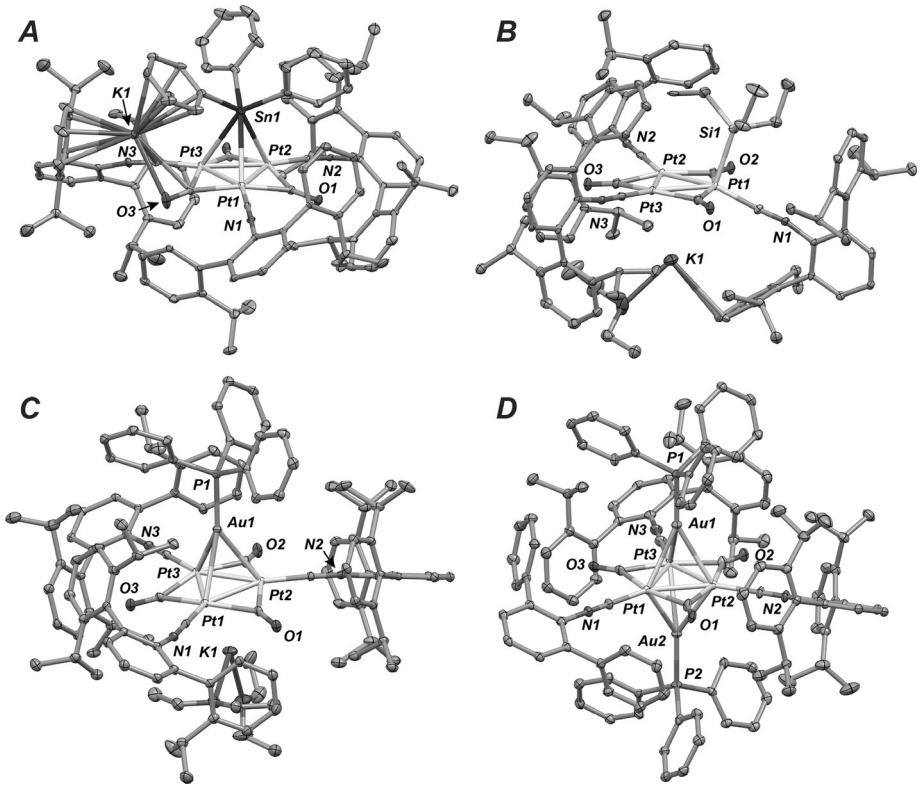

Figure 3. Molecular structure of A) $K[Pt_3(\mu_3\text{-}SnPh_3)(\mu\text{-}CO)_3(CNAr^{Dipp2})_3]$ (**2**), B) $K(Et_2O)[Pt_3(SiEt_3)(\mu\text{-}CO)_3(CNAr^{Dipp2})_3]$ (**3**), C) $K(Et_2O)_2[Pt_3(\mu_3\text{-}AuPPh_3)(\mu\text{-}CO)_3(CNAr^{Dipp2})_3]$ (**4**), and D) $Pt_3(\mu_3\text{-}AuPPh_3)_2(\mu\text{-}CO)_3(CNAr^{Dipp2})_3$ (**5**). Some *i*Pr groups have been removed for clarity.

nostannyl ligands.[43] Contrastingly, the triethylsilyl ligand in **3** is terminally bound to a single Pt center, with the Pt–Si bond vector being nearly orthogonal to the Pt_3 plane. The isocyanide bound to the silyl-ligated platinum center bends significantly out of the plane toward the opposite face of the cluster. However, despite the asymmetry evident in the solid-state structure of **3**, only a single sharp set of -Ar^{Dipp2} resonances are detected by ^{1}H NMR spectroscopy at 20 °C, indicating that exchange of the silyl ligand between the three Pt centers is fast on the NMR timescale. Dianionic K_2[**1**] also reacts with one or two equivalents of $AuCl(PPh_3)$, providing dark blue $K(Et_2O)_2[Pt_3(\mu_3\text{-}AuPPh_3)(\mu\text{-}CO)_3(CNAr^{Dipp2})_3]$ (**4**, Figure 3C) or forest green $Pt_3(\mu_3\text{-}AuPPh_3)_2(\mu\text{-}CO)_3(CNAr^{Dipp2})_3$ (**5**, Figure 3D). In both clusters, the -$AuPPh_3$ fragments symmetrically bridge the three Pt centers affording a Pt_3Au tetrahedron (**4**) or a Pt_3Au_2 trigonal bipyramid (**5**). While reminiscent of the formation of $[Pt_3(\mu_3\text{-}AuPCy_3)(\mu\text{-}CO)_3(PCy_3)_3]^+$, which is produced by capping the corresponding neutral Pt_3 cluster with a $[AuPCy_3]^+$ fragment,[44] it should be noted that the two additional valence electrons possessed by K_2[**1**] compared to $Pt_3(\mu\text{-}CO)_3(PCy_3)_3$ allows for the isolation of an anionic Pt/Au cluster, of which only one other structurally characterized example is known.[45] These extra electrons also allow for the formation of **5** via addition of a second equivalent of $[AuPPh_3]^+$, a transformation which is not accessible to $[Pt_3(\mu_3\text{-}AuPCy_3)(\mu\text{-}CO)_3(PCy_3)_3]^+$[46] and has not been reported for any phosphine-substituted $Pt_3(\mu\text{-}CO)_3(PR_3)_3$ cluster. Accordingly, these reactions leading to the formation of complexes **2**–**5** demonstrate that while e^- equivalents are housed in the ligand-based π^* manifold of K_2[**1**], electrophilic functionalization can proceed at the platinum centers of the *triangulo*-Pt_3 core.

In conclusion, the kinetic stabilization afforded by encumbering *m*-terphenyl isocyanides, in concert with their isolobal relationship to CO, allows for the isolation of a robust analogue to Chini's $[Pt_3(CO)_6]^{2-}$ dianion. Remarkably, the corresponding monoanion is also isolable and was shown to contain one unpaired electron located primarily on the aggregate ligand π^* system. Importantly, this study provides precedent for a set of isocyanide and carbonyl ligands to act in a redox non-innocent fashion. We are exploring additional reactivity patterns of these Pt_3 clusters that harness this unique electronic structure feature.

Acknowledgements

We are grateful to the U.S. National Science Foundation (CHE-1464978) for support of this work and for a Graduate Research Fellowship to B.R.B. We thank Dr. Mohand Melaimi for assistance with cyclic voltammetry measurements, as well as Prof. Michael J. Tauber and Douglas W. Agnew for assistance with EPR measurements. The W. M. Keck Foundation is also gratefully acknowledged for use of computing resources at the W. M. Keck Laboratory for Integrated Biology II. J.S.F is a Camille Dreyfus Teacher-Scholar (2012-2017).

Keywords: cluster compounds · isocyanides · non-innocent ligands · platinum

How to cite: *Angew. Chem. Int. Ed.* **2016**, *55*, 9253–9258
Angew. Chem. **2016**, *128*, 9399–9404

[1] E. W. Abel, F. G. A. Stone, *Q. Rev. Chem. Soc.* **1970**, *24*, 498.
[2] J. P. Collman, *Acc. Chem. Res.* **1975**, *8*, 342.
[3] J. E. Ellis, in *Advances in Organometallic Chemistry, Vol. 31* (Eds.: F. G. A. Stone, R. West), Academic Press, San Diego, **1990**, p. 1.
[4] J. E. Ellis, *Organometallics* **2003**, *22*, 3322–3338.
[5] H. Behrens, in *Advances in Organometallic Chemistry, Vol. 18,* (Eds.: F. G. A. Stone, R. West), Academic Press, San Diego, **1980**, p. 1.
[6] P. Chini, *J. Organomet. Chem.* **1980**, *200*, 37.
[7] J. C. Calabrese, L. F. Dahl, P. Chini, G. Longoni, S. Martinengo, *J. Am. Chem. Soc.* **1974**, *96*, 2614.
[8] G. Longoni, P. Chini, *J. Am. Chem. Soc.* **1976**, *98*, 7225.

[9] C. Femoni, F. Kaswalder, M. C. Iapalucci, G. Longoni, M. Mehlstäubl, S. Zacchini, A. Ceriotti, *Angew. Chem. Int. Ed.* **2006**, *45*, 2060; *Angew. Chem.* **2006**, *118*, 2114.
[10] C. Femoni, F. Kaswalder, M. C. Iapalucci, G. Longoni, S. Zacchini, *Eur. J. Inorg. Chem.* **2007**, 1483.
[11] C. Femoni, M. C. Iapalucci, G. Longoni, T. Lovato, S. Stagni, S. Zacchini, *Inorg. Chem.* **2010**, *49*, 5992.
[12] P. Greco, M. Cavallini, P. Stoliar, S. D. Quiroga, S. Dutta, S. Zacchini, M. C. Iapalucci, V. Morandi, S. Milita, P. G. Merli, F. Biscarini, *J. Am. Chem. Soc.* **2008**, *130*, 1177.
[13] D. A. Serban, P. Greco, S. Melinte, A. Vlad, C. A. Dutu, S. Zacchini, M. C. Iapalucci, F. Biscarini, M. Cavallini, *Small* **2009**, *5*, 1117.
[14] S. Zacchini, *Eur. J. Inorg. Chem.* **2011**, 4125.
[15] C. Femoni, F. Kaswalder, M. C. Iapalucci, G. Longoni, M. Mehlstäubl, S. Zacchini, *Chem. Commun.* **2005**, 5769.
[16] A. Albinati, *Inorg. Chim. Acta* **1977**, *22*, L31.
[17] T. Yoshida, S. Otsuka, *J. Am. Chem. Soc.* **1977**, *99*, 2134.
[18] R. A. Burrow, D. H. Farrar, J. J. Irwin, *Inorg. Chim. Acta* **1991**, *181*, 65.
[19] L. Ortega-Moreno, R. Peloso, C. Maya, A. Suárez, E. Carmona, *Chem. Commun.* **2015**, *51*, 17008.
[20] E. Poverenov, M. Gandelman, L. J. W. Shimon, H. Rozenberg, Y. Ben-David, D. Milstein, *Organometallics* **2005**, *24*, 1082.
[21] For ligand substitution studies of $[Pt_3(CO)_6]_n^{2-}$ ($n=2-6$) with PPh_3 to give mixed carbonyl/phosphine anionic oligomers, see: I. Ciabatti, C. Femoni, M. C. Iapalucci, G. Longoni, T. Lovato, S. Zacchini, *Inorg. Chem.* **2013**, *52*, 4384.
[22] G. W. Margulieux, N. Weidemann, D. C. Lacy, C. E. Moore, A. L. Rheingold, J. S. Figueroa, *J. Am. Chem. Soc.* **2010**, *132*, 5033.
[23] M. A. Stewart, C. E. Moore, T. B. Ditri, L. A. Labios, A. L. Rheingold, J. S. Figueroa, *Chem. Commun.* **2011**, *47*, 406.
[24] A. E. Carpenter, G. W. Margulieux, M. D. Millard, C. E. Moore, N. Weidemann, A. L. Rheingold, J. S. Figueroa, *Angew. Chem. Int. Ed.* **2012**, *51*, 9412; *Angew. Chem.* **2012**, *124*, 9546.
[25] C. C. Mokhtarzadeh, G. W. Margulieux, A. E. Carpenter, N. Weidemann, C. E. Moore, A. L. Rheingold, J. S. Figueroa, *Inorg. Chem.* **2015**, *54*, 5579.
[26] W. Kaim, *Inorg. Chem.* **2011**, *50*, 9752.
[27] C. Pierpont, *Coord. Chem. Rev.* **2001**, *216–217*, 99.
[28] R. Eisenberg, H. B. Gray, *Inorg. Chem.* **2011**, *50*, 9741.
[29] B. R. Barnett, C. E. Moore, A. L. Rheingold, J. S. Figueroa, *J. Am. Chem. Soc.* **2014**, *136*, 10262.
[30] B. R. Barnett, C. E. Moore, P. Chandrasekaran, S. Sproules, A. L. Rheingold, S. DeBeer, J. S. Figueroa, *Chem. Sci.* **2015**, *6*, 7169.
[31] B. M. Still, P. G. A. Kumar, J. R. Aldrich-Wright, W. S. Price, *Chem. Soc. Rev.* **2007**, *36*, 665.
[32] P. Archirel, *J. Phys. Chem. C* **2016**, *120*, 8343.
[33] P. Arrizabalaga, P. Castan, M. Geoffroy, J. P. Laurent, *Inorg. Chem.* **1985**, *24*, 3656.
[34] J. Matsunami, H. Urata, K. Matsumoto, *Inorg. Chem.* **1995**, *34*, 202.
[35] T. Schmauke, E. Möller, E. Roduner, *Chem. Commun.* **1998**, 2589.
[36] P. S. Braterman, J.-I. Song, C. Vogler, W. Kaim, *Inorg. Chem.* **1992**, *31*, 222.
[37] B. Hirani, J. Li, P. I. Djurovich, M. Yousufuddin, J. Oxgaard, P. Persson, S. R. Wilson, R. Bau, W. A. Goddard, M. E. Thompson, *Inorg. Chem.* **2007**, *46*, 3865.
[38] Percent orbital contributions are reported as the Löwdin reduced orbital populations.
[39] J. W. Lauher, *J. Am. Chem. Soc.* **1978**, *100*, 5305.
[40] D. J. Underwood, R. Hoffmann, K. Tatsumi, A. Nakamura, Y. Yamamoto, *J. Am. Chem. Soc.* **1985**, *107*, 5968.
[41] C. Mealli, *J. Am. Chem. Soc.* **1985**, *107*, 2245.
[42] While a detailed analysis of the Pt–Pt bonding situation in *triangulo*-Pt_3 clusters is outside the scope of this text, it has been examined with EHMO calculations and discussed at length elsewhere. See Refs. [39–41], also: D. I. Gilmour, D. M. P. Mingos, *J. Organomet. Chem.* **1986**, *302*, 127.
[43] Cambridge Structural Database (CSD), version 5.37 (November **2015**).
[44] C. E. Briant, R. W. M. Wardle, D. M. P. Mingos, *J. Organomet. Chem.* **1984**, *267*, c49.
[45] A. Ceriotti, P. Macchi, A. Sironi, S. El Afefey, M. Daghetta, S. Fedi, F. F. de Biani, R. Della Pergola, *Inorg. Chem.* **2013**, *52*, 1960.
[46] D. M. P. Mingos, P. Oster, D. J. Sherman, *J. Organomet. Chem.* **1987**, *320*, 257.

Received: May 19, 2016
Published online: June 27, 2016

